19ENG05 NanoWires

Good practice guide No. 4

Quantitative nanomaterial testing using quasi-static and dynamic AFM methods

Lead partner: PTB

Due date of the deliverable: 31.08.2023

Actual submission date of the deliverable: 30.11.2023

This project has received funding from the EMPIR programme co-financed by the Participating States and from the European Union's Horizon 2020 research and innovation programme.

EMPIR EURAMET
The EMPIR initiative is co-funded by the European Union's Horizon 2020 research and innovation programme and the EMPIR Participating States

The EMPIR initiative is co-funded by the European Union's Horizon 2020 research and innovation programme and the EMPIR Participating States

Content

EMPIR
The EMPIR initiative is co-funded by the European Union's Horizon 2020 research and innovation programme and the EMPIR Participating States
EURAMET

1. Introduction

To date, atomic force microscopes (AFM) [1-2] have been frequently used for nanomechanical measurement of small volumes of materials including ultrathin layers and free-standing nanowires (NW), mainly owing to their extremely high force sensitivity up to pN range and high lateral resolution down to sub-10 nm. Different AFM nanomechanical methods have been developed, including quasi-static approaches, e.g. AFM nanoindentation, and dynamic approaches including nano-DMA and contact resonance (CR) AFM for measurement of elastic properties of nanomaterials [3].

In comparison with traditional nanomechanical measurements using nanoindentation instruments, where the measurement procedure, instrument calibration, measurement data evaluation, and uncertainty analysis have been well standardized with ISO 14577 [4-5], the reliability and accuracy of AFM nanomechanical measurements suffer, to large extent, to the poorly modelled tip area function of AFM tips in use.

In this good practice guide, we propose to **use reference bulk polymer to characterize the tip area function of AFM probes** for quantitative quasi-static AFM nanomechanical measurement, and dynamic AFM approaches as well.

2. Reference sample preparation

Typically, three polymer reference samples including polycarbonate (PC), polyamide-nylon 6 (PA) and low-density polyethylene (LDPE) are recommended to the consortium, mainly because their elastic properties range from several GPa down to several hundreds MPa, offer therefore tip characterization down to several hundred nanometers even for moderate indentation force F_p up to 1000 µN.

These bulk polymers can be ordered from Goodfellow GmbH in the shape of sheets with a thickness of 5 mm. For the sake of material testing, flat samples with in-plane dimensions of 10 mm by 5 mm are cut from these polymer sheets.

These polymer samples are thereafter glued onto metal plates, which can then be magnetically held onto the sample stages of a nanoindentation instrument and the experimental setup of MEMS nanoindenter, respectively.

A commercial AFM is used to determine the surface roughness of these three samples, as shown in Fig. 1. The average surface roughness Sa of PC sample is found to be about 8 nm, and the surfaces of PA and LDPE have the average roughness Sa of about 23 nm and 56 nm, respectively.

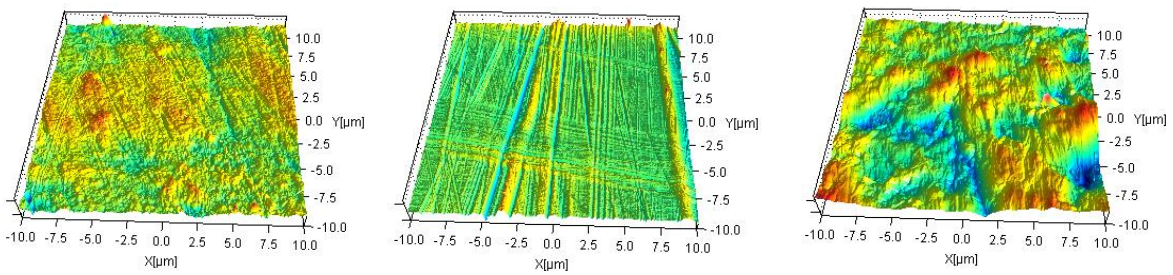

(a) (b) (c)

GPG-Figure 1 AFM measurements of the surface roughess of reference polymer samples: (a) PA, (B) PC, (c) LDPE

3. Determination of the mechanical properties of reference bulk polymers using a commercial nanoindentation instrument

To determine the mechanical properties of these bulk polymers, a commercial nanoindentation instrument (Hysitron Triboindenter TI-950) equipped with a diamond Berkovich indenter has been used.

3.1 Testing procedure and data evaluation

Depth-controlled nanoindentation tests have been performed for the three samples. Within the centre area of each sample, a matrix (N x N) of nanoindentations have been made. And the typical testing procedure of each nanoindentation test is as follows:

1) The Berkovich Indenter is firstly engaged onto the sample surface with a preload of 2 μN, and then
2) lifted 100 nm away from the surface,
3) re-approaches and makes three-segmented nanoindentation on the sample surface.

Each nanoindentation cycle consists of a loading, a holding and an unloading segment with the loading time t_{load}, holding duration t_{hold} and unloading time t_{unload}, respectively, as shown in S-Fig. 1.

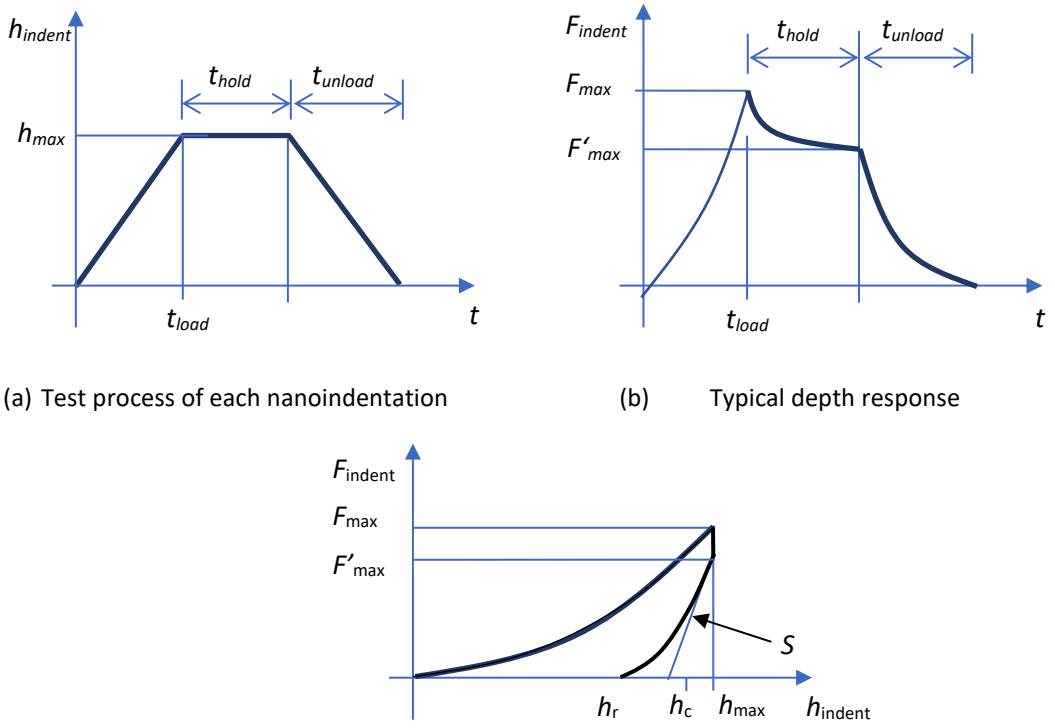

(a) Test process of each nanoindentation

(b) Typical depth response

(c) Data evaluation

GPG-Figure 2 Data evaluation for nanoindentation measurements in accordance with ISO 14577-1

The data evaluation is prescribed by the ISO 14577-1, i.e. the contact depth h_c is firstly calculated from the unloading curve, the reduced indentation modulus E_r of the sample is then deduced from the slope S of the unloading curve and the contact area A_c at h_c, and the indentation hardness H_{IT} is defined as F'_{max}/A_c, where F'_{max} corresponds to the indentation force F_{indent} at the starting point of unloading procedure.

$$h_c = h_{\max} - \varepsilon \frac{F_{\max}}{S} \quad (1)$$

$$E_r = \frac{\sqrt{\pi}}{2} \frac{S}{\sqrt{A_c}} \quad (2)$$

$$H_{IT} = \frac{F_{\max}}{A_c} \quad (3)$$

It is worthwhile to mention that here the coefficient $\varepsilon = 0.75$. To derive the contact stiffness S at the starting point of unloading procedure, the upper part (typically 30 – 98 % of $F'_{\max}$) of the measurement data of unloading curves is fitted into the power law function $F = \alpha \cdot (h - h_f)^m$. Finally, we have

$$S|_{h=h_{\max}} = \hat{m} \cdot \hat{\alpha} \left(h_{\max} - \hat{h}_f\right)^{\hat{m}-1} \quad . \quad (4)$$

3.2 Calibration results

One of the typical indentation curves obtained for bulk PC is shown in Fig. 3. The measured indentation curves obtained by the array indentations on different materials are shown in Fig. 4. It is noticeable that the measurement data for PA and LDPE look quite noisy, since these two bulk samples have quite rough surfaces.

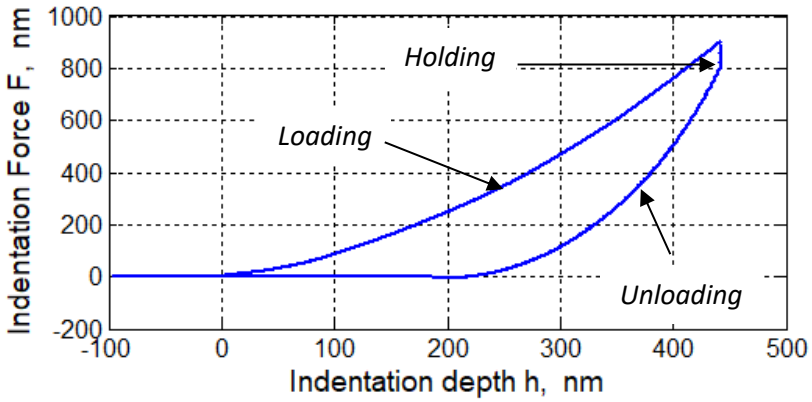

GPG-Figure 3. One of the typical depth-controlled indentation depth-force curves for a bulk polycarbonate sample obtained with a Berkovich indenter. And $t_{load} = t_{unload} = 35$ s, $t_{hold} = 15$ s.

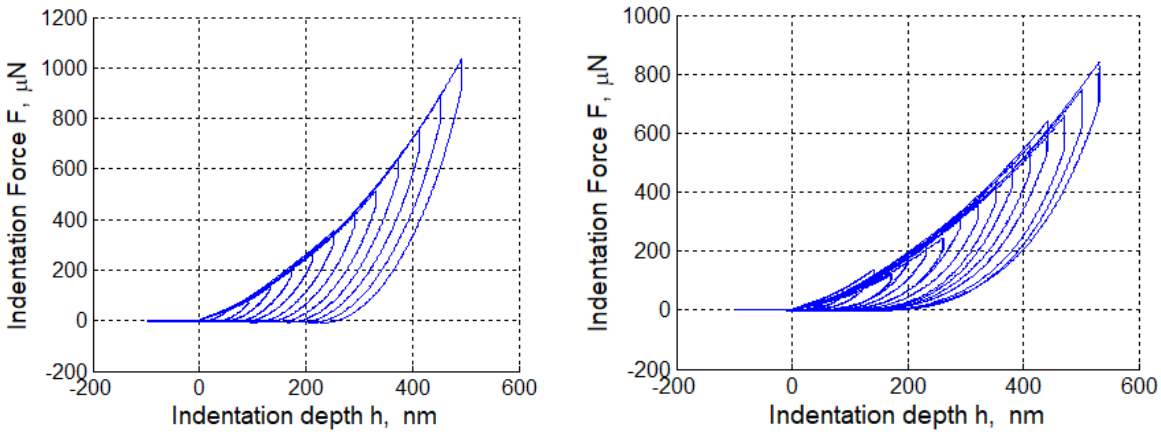

(a) Multi-indentation curves on PC

(b) Multi-indentation curves on PA

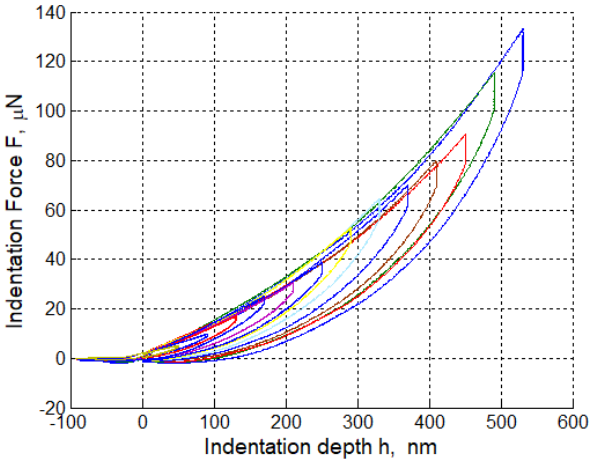

(c) Multi-indentation curves on LDPE

GPG-Figure 4. Typical depth-controlled indentation depth-force curves obtained by array indentation on different polymers (Berkovich indenter, $t_{load} = t_{unload} = 35$ s, $t_{hold} = 15$ s).

Under the measurement conditions of $t_{load} = t_{unload} = 35$ s, $t_{ho.ld} = 15$ s, the mechanical properties of bulk PC, PA and LDPE determined by the nanoindentation instrument are illustrated in Fig. 5.

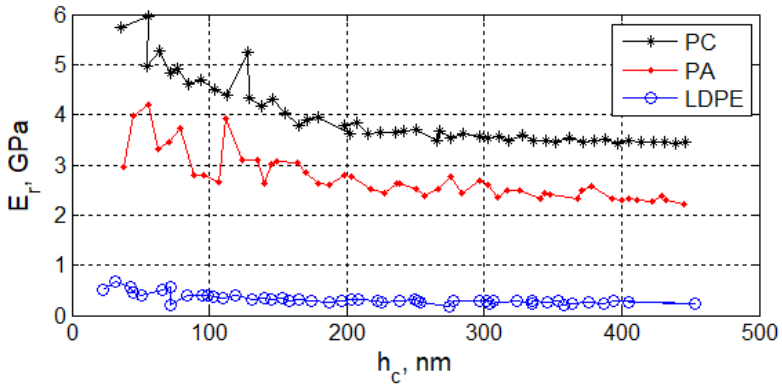

(a) Measured reduced indentation moduli of three polymers with respect to the contact depth h_c

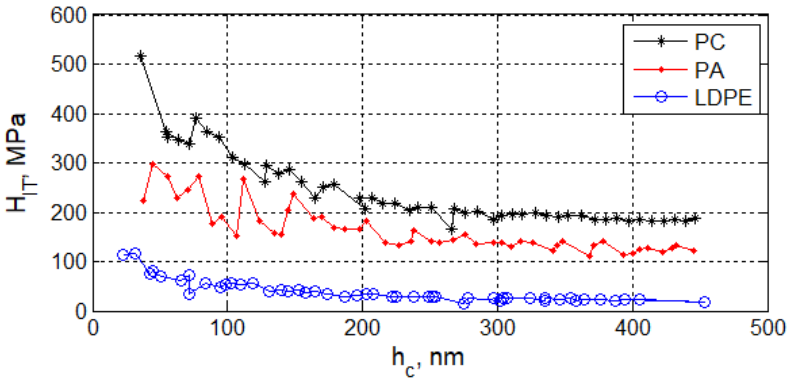

(b) Measured indentation hardness of three polymers with respect to the contact depth h_c

GPG-Figure 5 Fundamental mechanical properties (reduced indentation modulus E_r and hardness H_{IT}) of three bulk polymers (PC, PA and LDPE)

It can be seen from Fig. 5 that the mechanical properties of these three polymers measured by nanoindentation technique tend to be stable, when the contact depth $h_c \geq 250$ nm. The mean values of the three polymers' mechanical properties for $h_c \geq 250$ nm are listed in Table 1.

Materials, Measurement conditions	PC ($h_c > 250$ nm)		PA ($h_c > 250$ nm)		LDPE ($h_c > 250$ nm)	
	Er, GPa	H_{IT}, MPa	Er, GPa	H_{IT}, MPa	Er, GPa	H_{IT}, MPa
$t_{load} = t_{unload} = 35$ s, $t_{hold} = 15$ s	3.6 ± 0.1	202 ± 22	2.5 ± 0.2	135 ± 15	0.27 ± 0.03	25 ± 5
$t_{load} = t_{unload} = 35$ s, $t_{hold} = 50$ s	3.7 ± 0.4	184 ± 20	2.3 ± 0.3	121 ± 25	0.26 ± 0.06	25 ± 6

GPG-Table 1. Mechanical properties of bulk PC, PA and LDPE measured by Hysitron Triboindenter TI-950 using a Berkovich indenter under different test procedures.

Being aware of the fact that polymer samples possess generally viscosity, a series of nanoindentation measurements with the measurement conditions of $t_{load} = t_{unload} = 35$ s, $t_{hold} = 50$ s have been performed. And the corresponding results are also listed in Table 1.

It can be seen that the bulk LDPE shows less viscosity, and its mechanical properties remains nearly constant, even when the holding time is nearly four times increased. However, the measured E_r and H_{IT} of bulk PC and PA will have about 10% variation, when t_{hold} is increased from 15 s to 50 s.

4. Quantitative nanomechanical measurements of bulk polymers using the MEMS nanoindenter with a silicon AFM probe

This GPG is focused on addressing one of the critical issues in quantitative AFM nanomechanical measurements, i.e. reliable characterization and modelling of the tip area function of AFM probes. To suppress the negative influences coming from traditional AFM instruments, in the following a MEMS-SPM platform [5] developed at PTB has been utilized for experimental investigation. This MEMS-SPM nanomechanical measurement system features high linearity of indentation force and high linearity and resolution for indentation depth measurement. Furthermore, various AFM probes with rectangular cantilever beams can be clamped by the MEMS-SPM head for material testing.

4.1 Tip area function characterization using reference polymers

A silicon AFM probe (Nanosensors™, PPP-NCHR) is clamped within the MEMS nanoindenter as an indenter for material testing. To perform nanomechanical measurements, the PC sample is first engaged onto the silicon AFM probe and then withdrawn from the probe until a predefined distance is reached (e.g. $h_0 = 50$ nm). Then, a typical 3-segmented depth-controlled nanoindentation procedure is followed: the pico-stage moves the sample at a constant speed within a time period t_{load} towards the AFM probe until a predefined position z_{max} is reached, holds the sample at z_{max} for a duration t_{hold} and then brings the sample back to its original position z_0 within the duration t_{unload}.

Figure 6(a) shows the typical depth-force curves for indentations in bulk PC under the conditions of t_{load} = t_{unload} = 35 s, t_{hold} = 50 s. For the measurement data 1 in Fig.6(a), the corresponding depth-time (*h*-*t*) and force-time (*F*-*t*) curves are also detailed in Fig. 6(b). It can be seen clearly from the *F*-*t* curve in Fig. 5(b) that, owing to relatively long holding time, the indentation force *F* has already become stable at the end of the holding period.

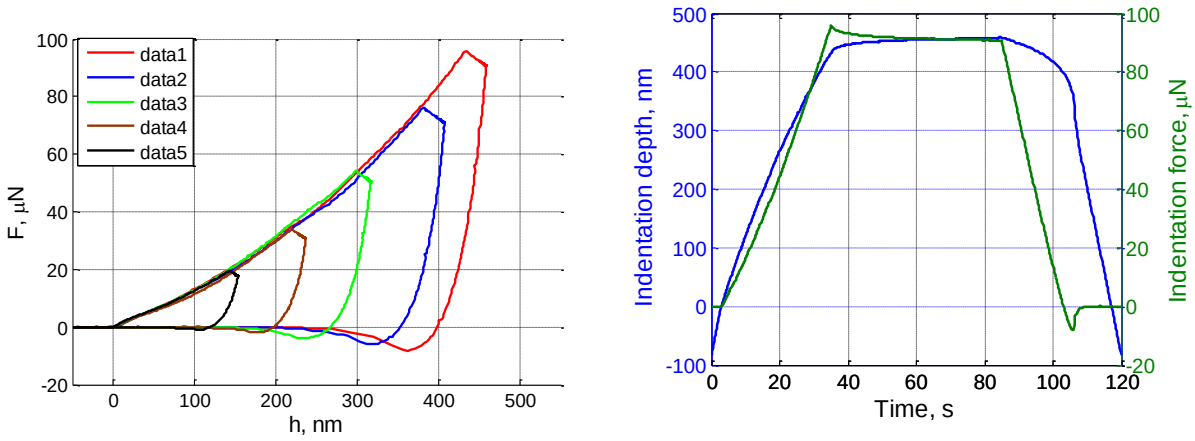

(a) Typical indentation curves for PC

(b) Indentation depth-time (*h*-*t*) and force-time (*F*-*t*) curves for measurement data1 in left figure.

GPG-Figure 6 Nanoindentation testing on bulk PC performed by the MEMS nanoindenter with a clamped silicon AFM probe

According to the Oliver-Pharr model [4], the contact depth h_c in Eq.(1) can be calculated as $h_c = h_{max} - \varepsilon F_{max}/S$. For the silicon AFM probes, $\varepsilon \approx 0.73$ [6].

The tip area function A_p of a silicon AFM probe in use is usually unknown. While the E_r of the reference PC has already been obtained in Section 3, the contact area A_p of this silicon probe can be deduced as $A_p = \pi/4 \cdot S^2/E_r^2$.

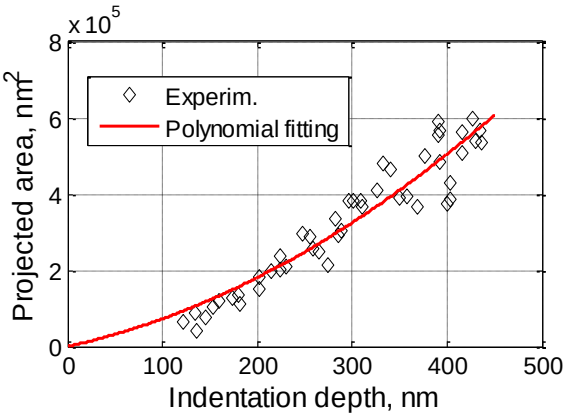

GPG-Figure 7 Tip area function of the silicon tip determined by the reference polymer PC

Following the measurement data evaluation above, we obtain the contact area A_p of the silicon tip as shown in Fig.7. Fitting the typical two-term AFM tip area function [6]

$$A_p = C_0 \cdot h_c^2 + C_1 \cdot h_c \quad (5)$$

to the measurement data, we obtain the tip area function of this silicon tip as $A_p = 1.78 \cdot h_c^2 + 548.04 \cdot h_c$. It should be noted that the term $C_0 = 1.78$ indicates the semi-apex angle of the silicon tip $\theta_{tip} = 37.0^{\circ}$.

Using Eq. (3), the hardness of PC is evaluated for the MEMS nanoindenter over the indentation depth h_c. The H_{IT} measured is found to be H_{IT} = (165 ± 7) MPa for h_c > 250 nm, which coincides well with the reference value obtained by means of other nanoindentation instruments.

4.2 Tip area function validation using reference polymer samples

Using the same MEMS nanoindenter and the identical test procedure detailed above, a series of indentation measurements on the bulk PA and LDPE have been performed. And the corresponding indentation depth-force curves are illustrated in Fig. 8(a) and 8(b), respectively. It is worthwhile to mention that, similar to the measurement data shown in Fig. 4(b) and 4(c), the measured indentation curves for bulk PA and LDPE look also quite noisy.

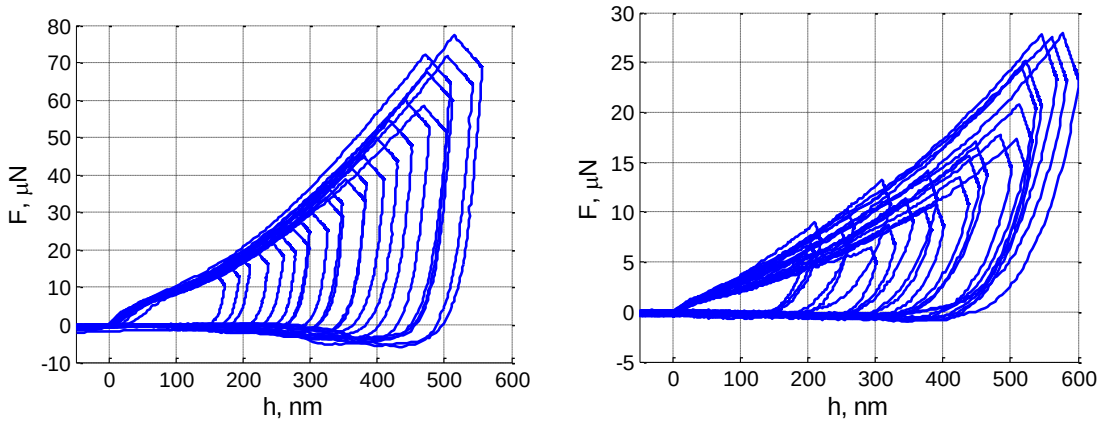

(a) Typical indentation curves for PA (b) Typical indentation curves for LDPE

GPG-Figure 8 Indentation depth-force curves for bulk PA and LDPE obtained by the MEMS nanoindenter with a clamped silicon AFM probe

Using this evaluated TAF in Subsection 4.1, the indentation curves shown in S-Fig. 6(a) and S-Fig. 6(b) have been analyzed to deduce the mechanical properties of bulk PA and PC, as shown in S-Fig. 7a and 7(b), respectively.

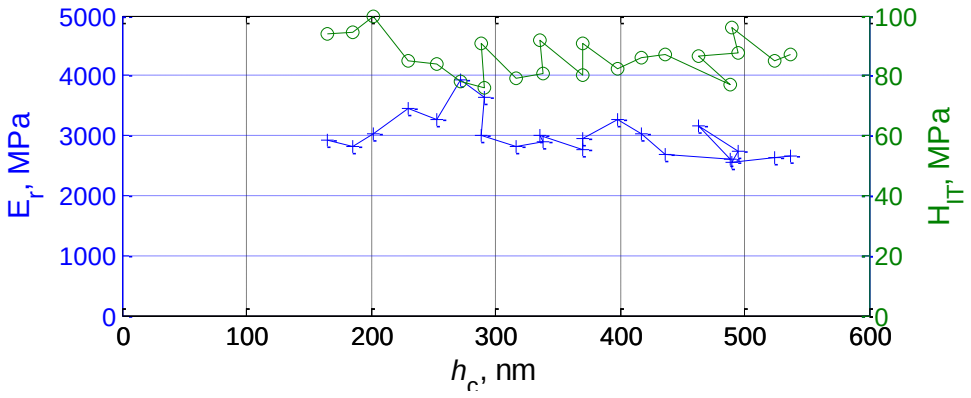

(a) Reduced elastic modulus E_r and indentation hardness H_{IT} of bulk PA evaluated from Fig. 8(a)

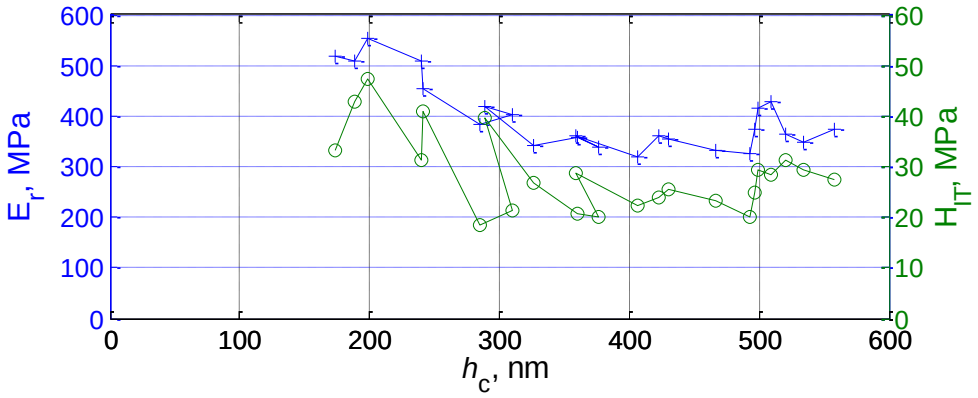

(b) Reduced elastic modulus E_r and indentation hardness H_{IT} of bulk LDPE evaluated from S-Fig. 8(b)

GPG-Figure 9 Indentation modulus and hardness of bulk PA and LDPE measured by the silicon AFM probe clamped in the MEMS nanoindenter

Finally, the averaged mechanical properties of bulk PC, PA and LDPE obtained by the MEMS nanoindenter are listed in Table 2.

Materials, Measurement conditions	PC (h_c > 250 nm)		PA (h_c > 250 nm)		LDPE (h_c > 250 nm)	
	Er, GPa	H_{IT}, MPa	Er, GPa	H_{IT}, MPa	Er, GPa	H_{IT}, MPa
t_{load} = t_{unload} = 35 s, t_{hold} = 50 s	* (Reference value for AFM tip characterisation)	165 ± 7	2.84 ± 0.22	85 ± 6	0.36 ± 0.03	25 ± 6

GPG-Table 2. Mechanical properties of bulk PC, PA and LDPE measured by the MEMS nanoindenter with a silicon AFM probe.

It can be clearly seen from Table 2 that reasonable mechanical properties of polymer samples can now be obtained, after the tip area function of the AFM probe is well determined.

5. Summary

In this good practice guide, one of the key issues in AFM based nanomechanical measurements, i.e. quantitative determination of the tip area function (TAF) of AFM probes, has been addressed.

Three reference bulk materials featuring relative smooth surface and less depth-dependent mechanical properties have been proposed for characterization of the TAF of AFM probes. Of course, polymer samples usually show ageing effect, therefore, the reference samples need to be regularly recalibrated using the measurement process and parameters detailed in **Section 3**.

Typically, the TAF of an AFM probe can be firstly characterized using the reference polymer PC, and thereafter be verified by the reference polymer PA and LDPE, as described in Section 4.

It is anticipated that quasi-static and dynamic AFM nanomechanical measurements using this GPG for the TAF characterization can achieve a measurement uncertainty of 10 %, under the condition that the stiffness of the AFM probes and the AFM instruments have been well calibrated [8].

References

[1] Fischer-Cripps A C 2006 Critical review of analysis and interpretation of nanoindentation test data *Surface and Coatings Technology* **200** 4153–4165.

[2] Griepentrog M, Krämer G, Cappella B 2013 Comparison of nanoindentation and AFM methods for the determination of mechanical properties of polymers Polymer Testing **32**(3) 455-460

[3] Killgore J P and DelRio F W 2018 Contact Resonance Force Microscopy for Viscoelastic Property Measurements: From Fundamentals to State-of-the-Art Applications *Macromolecules* **51**(18) 6977–6996

[4] Pharr G M and A Bolshakov A 2002 Understanding nanoindentation unloading curves *J Mater Res* **17** 2660-2671

[5] ISO 14577-1 (2002), Part 1: Test method.

[6] Passeri D, Bettucci A, *et al.* 2008 Quantitative measurement of indentation hardness and modulus of compliant materials by atomic force microscopy *Rev. Sci. Instrum.* **79** 066105

[7] Li Z, Gao S, Brand U, Hiller K and Wolff H 2020 A MEMS nanoindenter with an integrated AFM cantilever gripper for nanomechanical characterization of compliant materials *Nanotechnology* **31** 305502

[8] Brand U, Gao S, Engl W, et. al. 2017 Comparing AFM cantilever stiffness measured using the thermal vibration and the improved thermal vibration methods with that of an SI traceable method based on MEMS *Meas. Sci. Technol.* **28** 034010